

Nanoparticle Synthesis

Top-Down

via Attrition / Milling

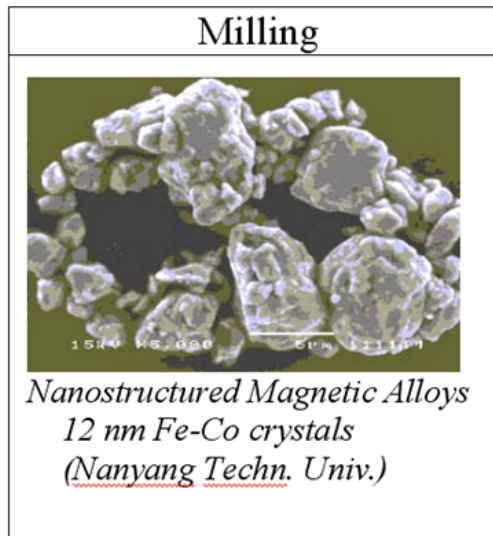
Involves mechanical thermal cycles

Yields

- broad size distribution (10-1000 nm)
- varied particle shape or geometry
- impurities

Application:

- Nanocomposites and
- Nano-grained bulk materials



Bottom-Up

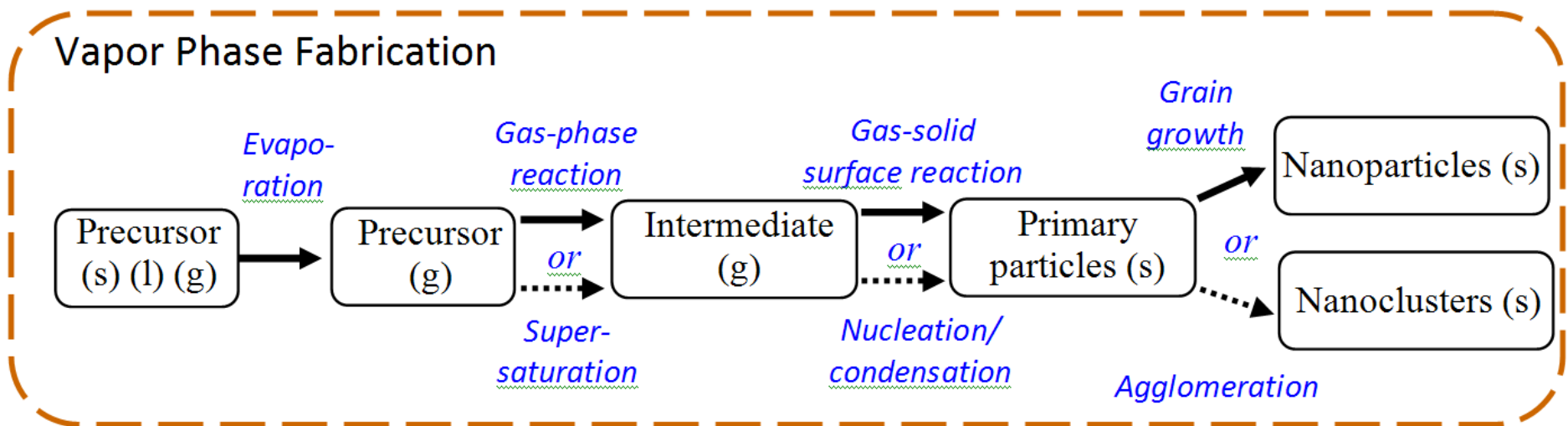
Via

- Pyrolysis
- Inert gas condensation
- Solvothermal Reaction
- Sol-gel Fabrication
- Structured Media

Bottom – Up Synthesis

Phase Classification:

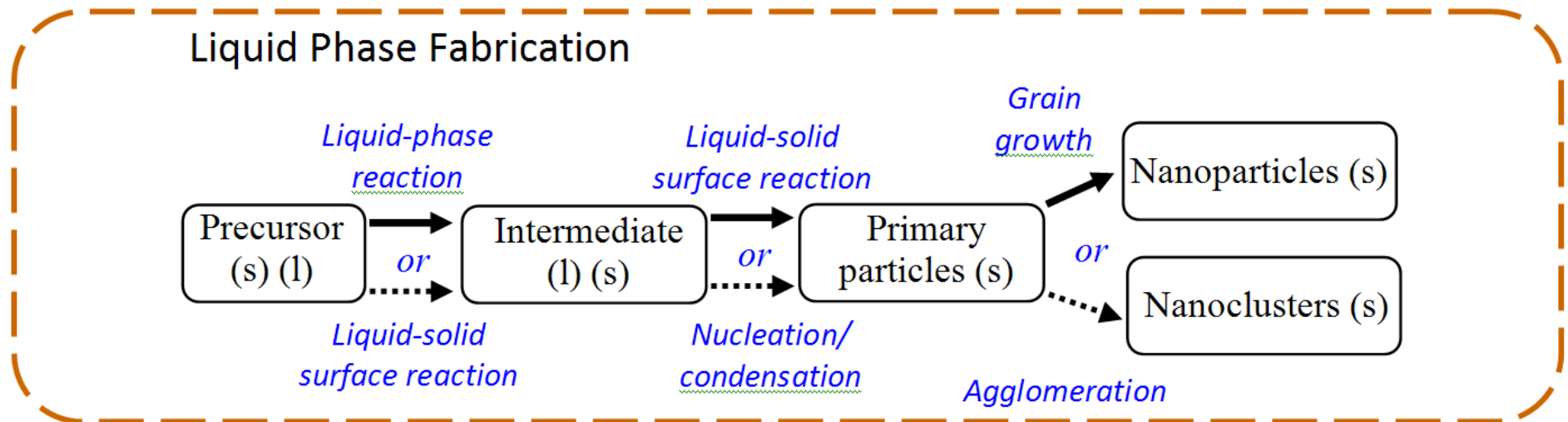
- I. Gas (Vapor) Phase Fabrication: *Pyrolysis, Inert Gas Condensation,*
- II. Liquid Phase Fabrication: *Solvothermal Reaction, Sol-gel, Micellar Structured Media*



Bottom – Up Synthesis

Phase Classification:

- I. Gas (Vapor) Phase Fabrication: *Pyrolysis, Inert Gas Condensation,*
- II. Liquid Phase Fabrication: *Solvothermal Reaction, Sol-gel, Micellar Structured Media*



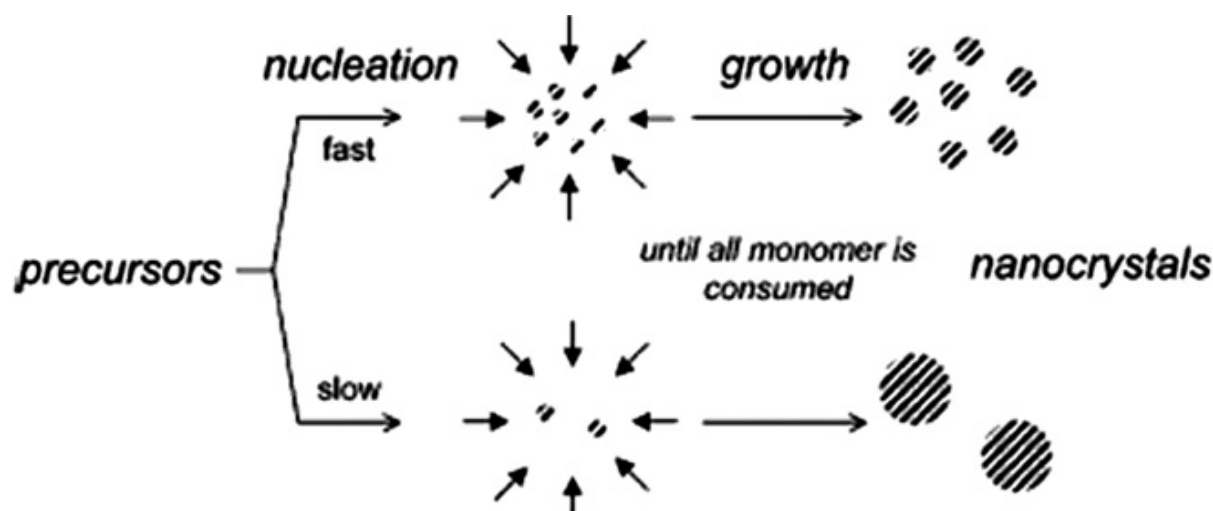
Homogeneous Condensation

Cluster free energy: *negative volume term* *positive surface term*

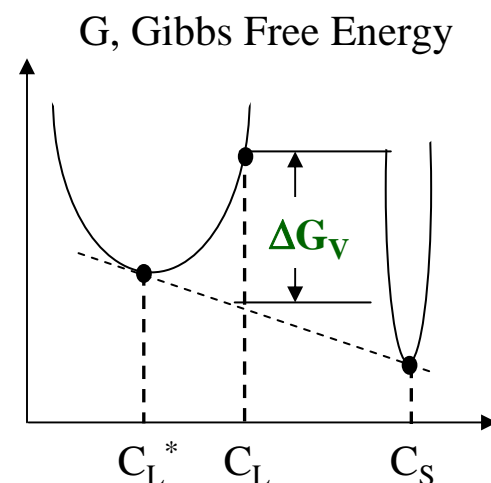
$$\Delta G^* = -\frac{4}{3}\pi r^3 \Delta G_v + 4\pi r^2 \gamma$$

Driving Force: ΔG_v

Bulk free energy difference
between old and new phase



E.E. Finney, R.G. Finke / J. Coll. Inter. Sci. **317** (2008) 351–374



Concentration:

C_L^* ... Solution in Equilibrium

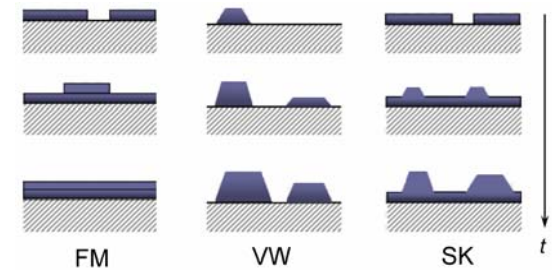
C_L ... Supersaturated Solution

C_S ... Solid phase

Growth Steps and Limitations

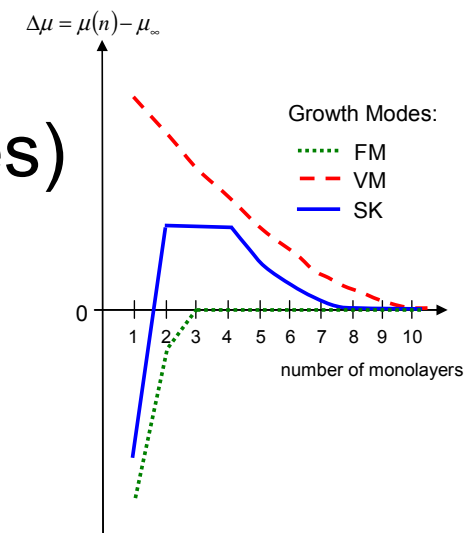
- Steps

- Generation of growth species (e.g., reduction from minerals)
- Diffusion from bulk to the growth surface
- Adsorption
- Surface growth (\rightarrow growth modes)



- Limitation

- Diffusion-limited growth
- Size-limited (Oswald ripening)
- Transport-limited growth



Vapor Phase Growth

Growth rate of vapor condensation:

$$R = \xi A_{NP} \frac{\Delta p}{\sqrt{2\pi m k_B T}}; \quad \text{Flux from gas kinetic theory}$$
$$\Delta p = p_V - p_e$$
$$\text{Spherical NP: } A_{NP} = 4\pi d_{NP}^2$$

ξ ... condensation coefficient (between 0 and 1)

A_{NP} ... surface area of condensate (nanoparticle NP)

m mass of gas molecule

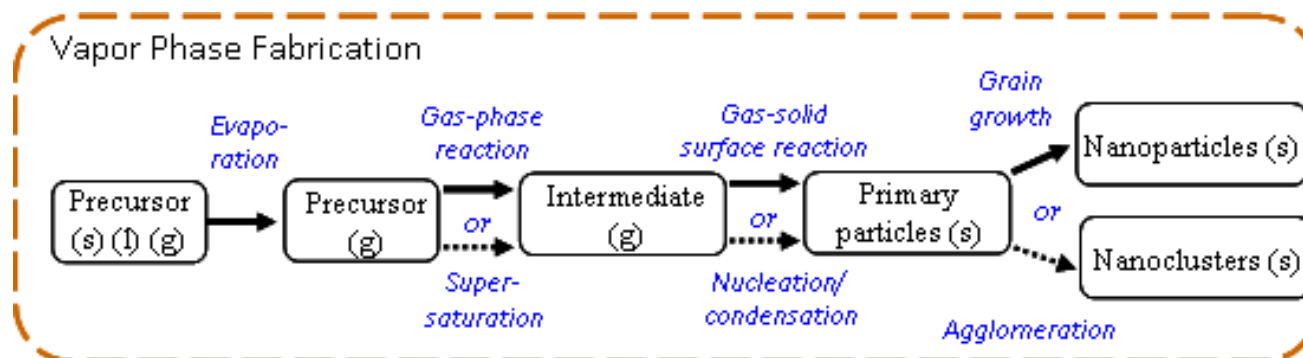
k_B Boltzmann constant, and T ... absolute temperature

Driving force: pressure difference Δp

p_V instantaneous vapor pressure

P_e local equilibrium pressure at the growing cluster

Mechanism and Effectiveness



- (i) precursor vaporization (typically involves a catalyst)
- (ii) nucleation, and
- (iii) growth stage

Effectiveness demands:

- simple process
- low cost
- continuous operation
- high yield

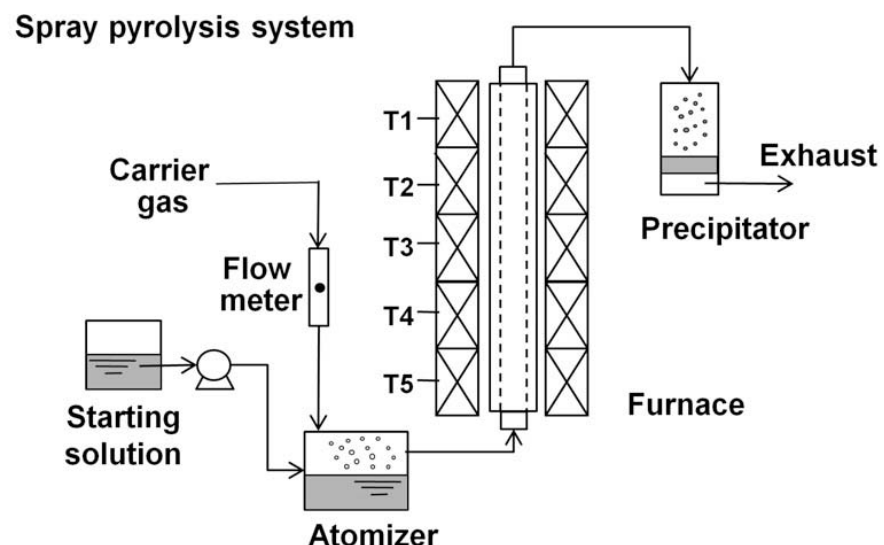
Aerosol Spray Methods
(e.g., Spray Pyrolysis)

Vapor Phase Synthesis Methods

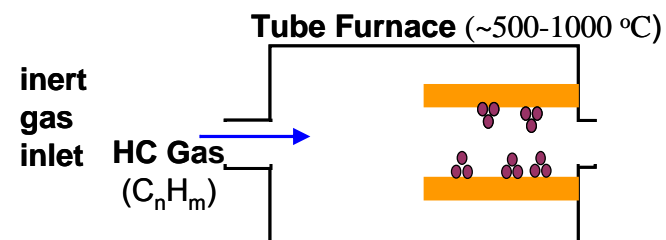
Discussed are:

- Pyrolysis
(Spray Pyrolysis)

Spray pyrolysis is the aerosol process that atomizes a solution and heats the droplets to produce solid particles

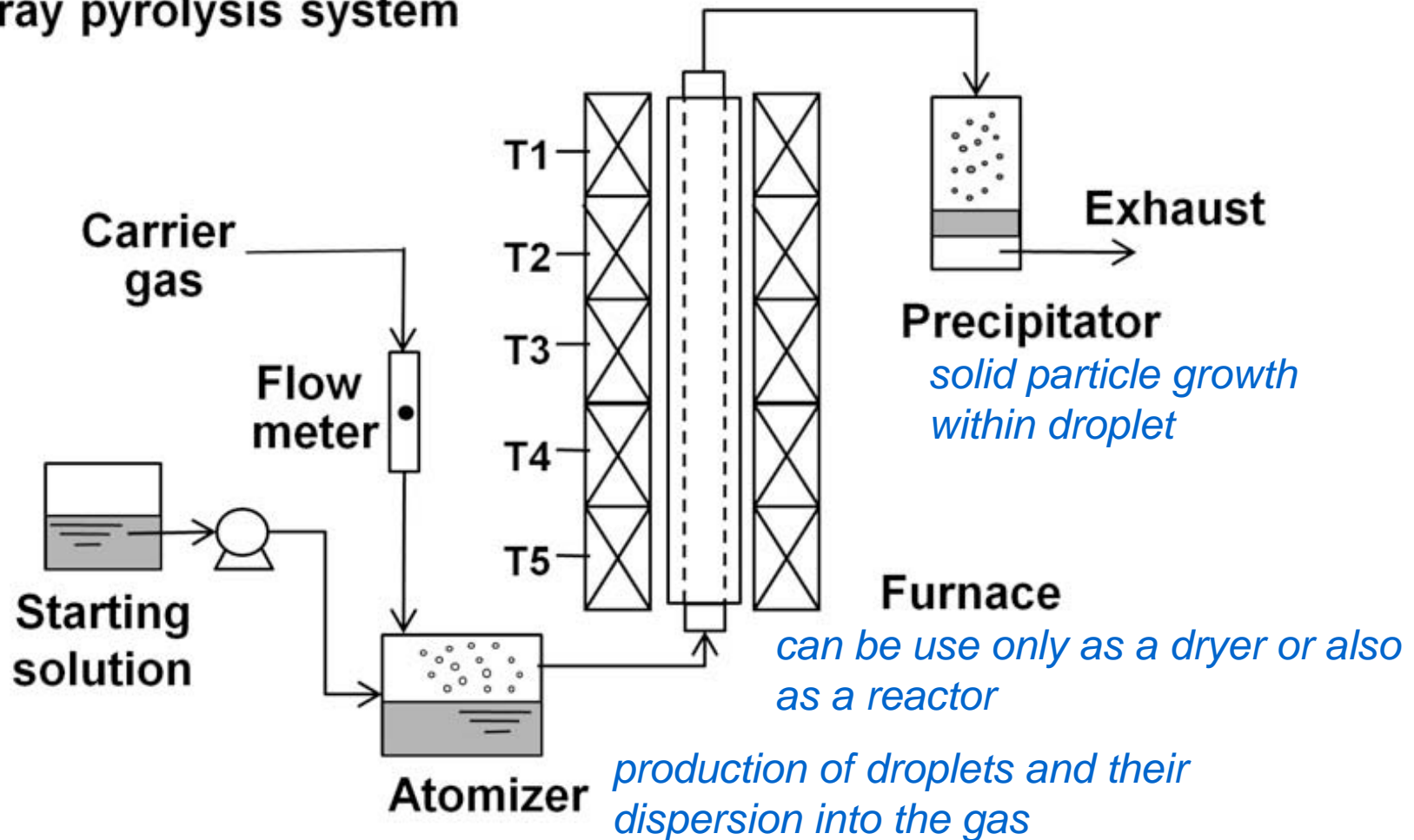


- Inert Gas Condensation
(Chemical Vapor Deposition)



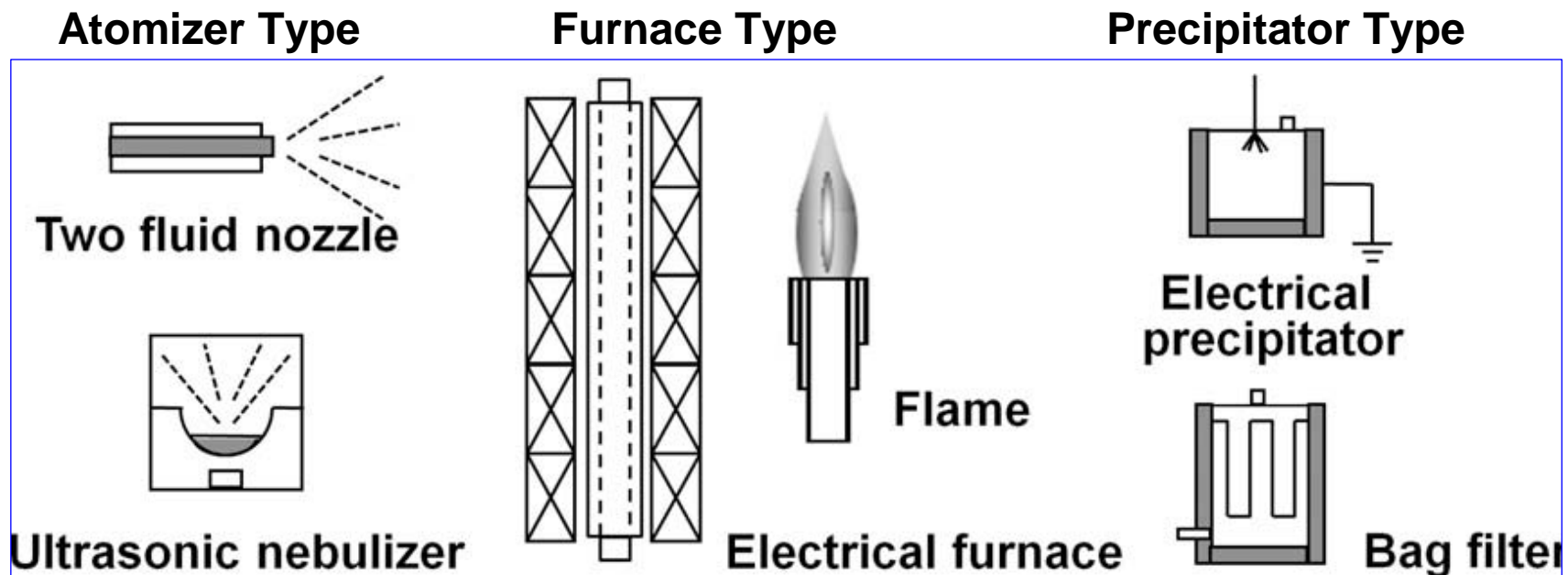
Spray Pyrolysis

Spray pyrolysis system



F. Iskandar, Adv. Powder Techn. **20** (2009) 283

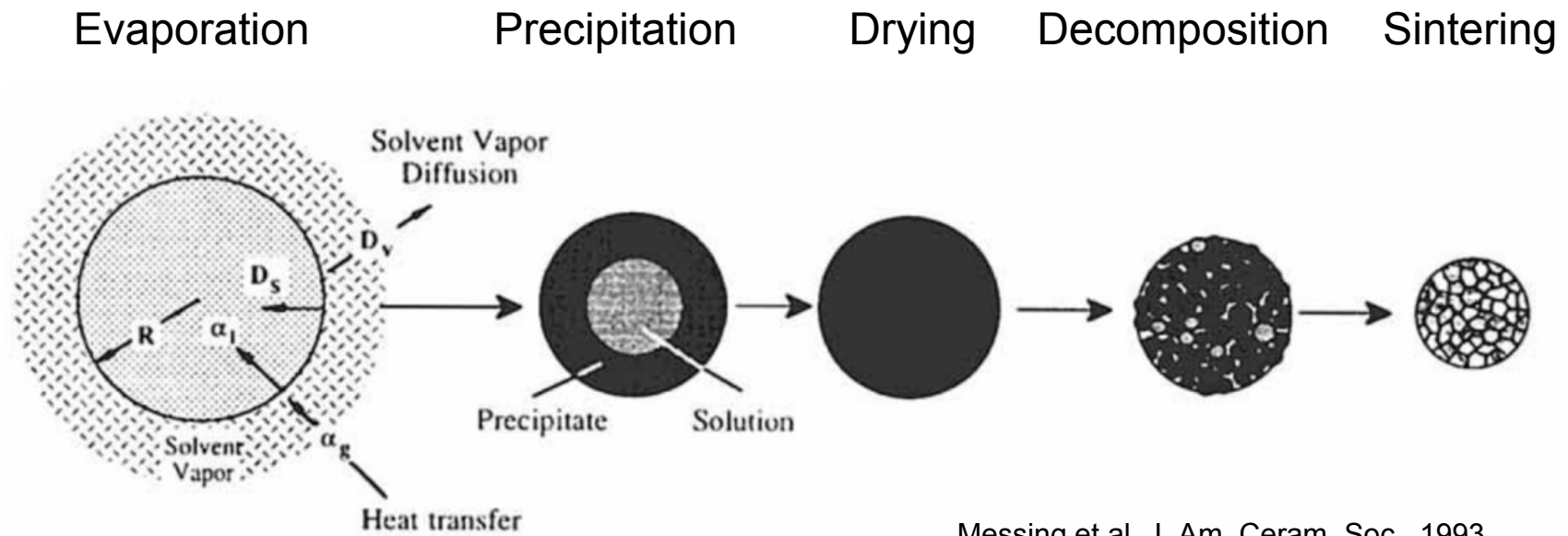
Spray Pyrolysis



F. Iskandar, Adv. Powder Techn. **20** (2009) 283

Spray Pyrolysis

Droplet Evolution

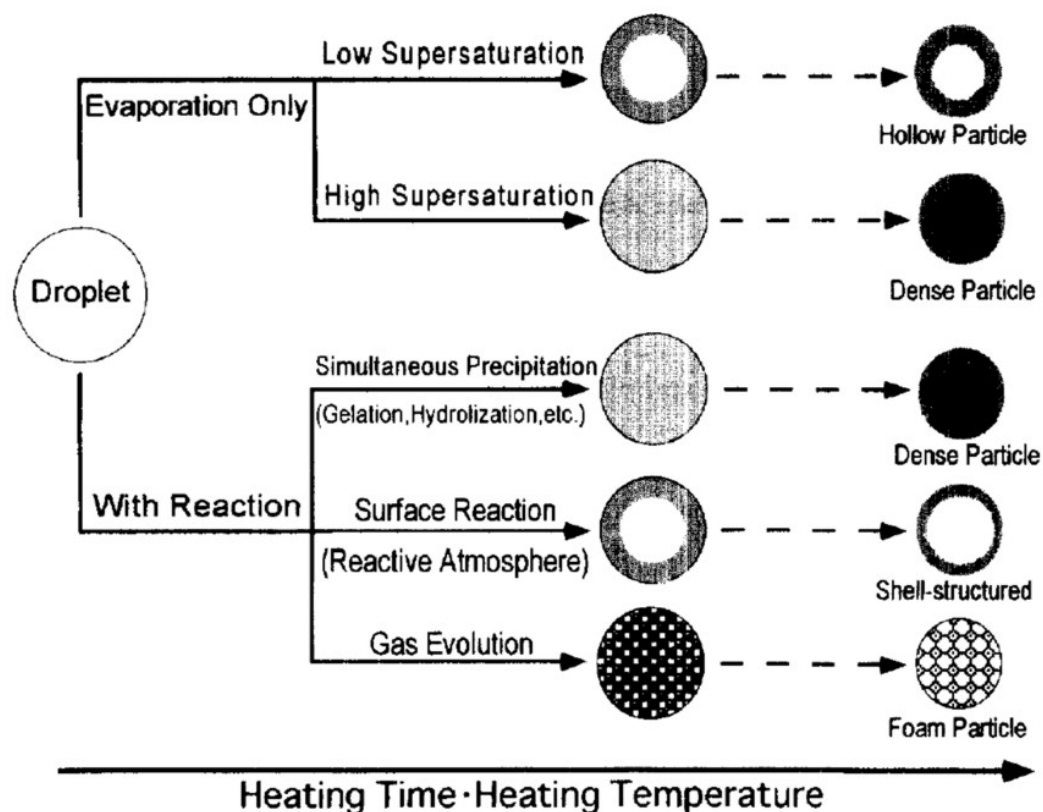


Messing et al, J. Am. Ceram. Soc., 1993

If the solute concentration at the center of the drop is less than the equilibrium saturation of the solute at the droplet temperature, then precipitation occurs only in that part of the drop where the concentration is higher than the equilibrium saturation, i.e., surface precipitation.

Spray Pyrolysis

Precipitation Control



Che et al, J. Aer. Sci., 1998

Messing et al, J. Am. Ceram. Soc., 1993

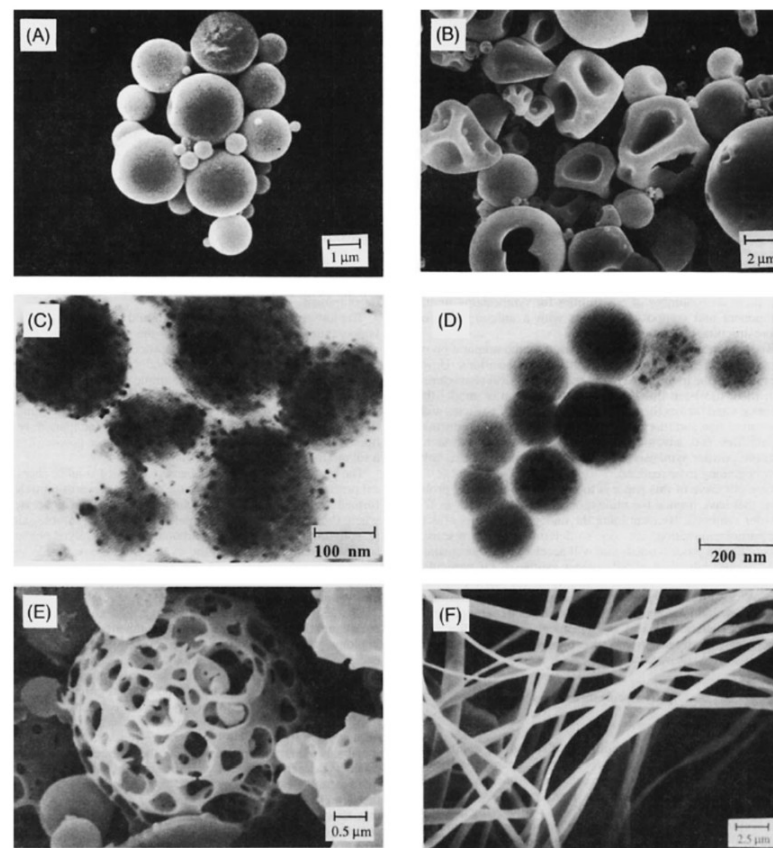
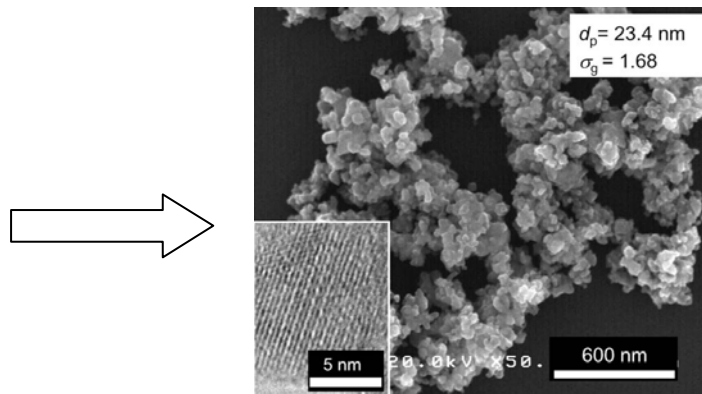
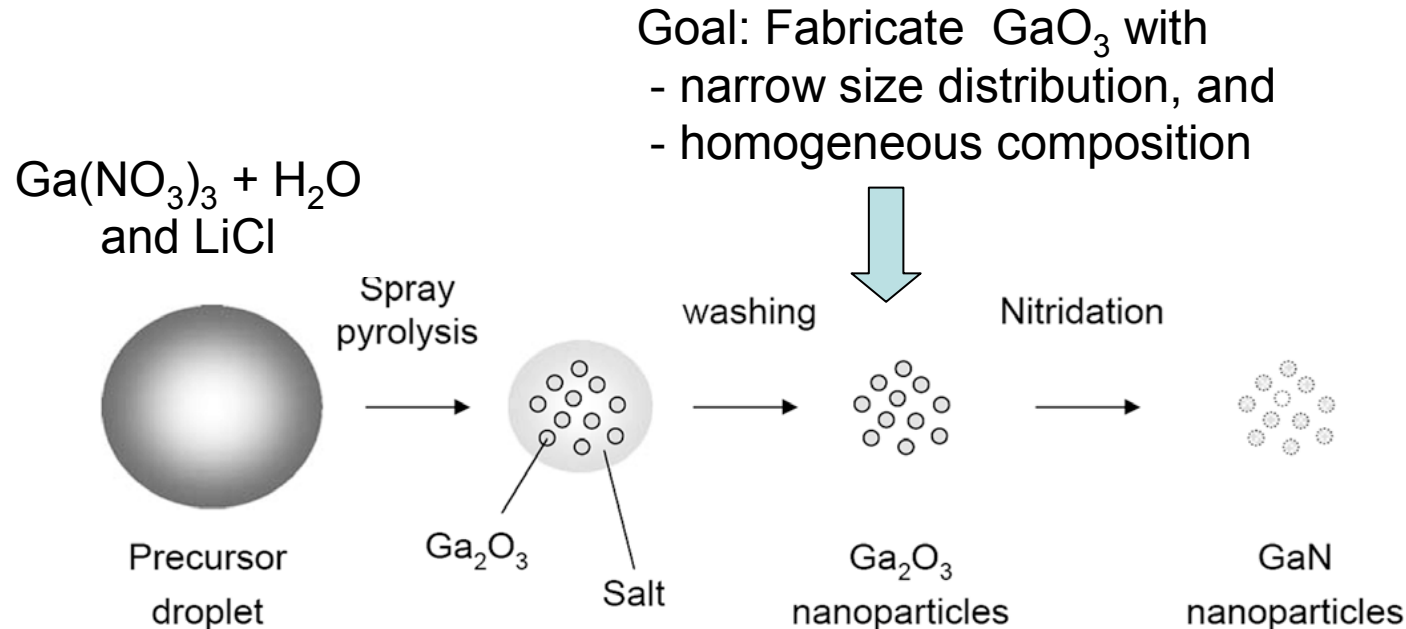


Fig. 3. Various morphologies of particles produced by SP processes: (A) solid ZrO_2 particles derived from 0.1 M ZHC solution, (B) irregular ZrO_2 particles derived from 1 M ZAC solution, (C) Al_2O_3 /platinum nanocomposite particles derived from 0.5 M $Al(OBu)_3$ -H₂PCl₄ solution, (D) Al_2O_3 /platinum nanocomposite particles derived from 0.5 M $Al(OBu)_3$ -H₂PCl₄ solution, (E) catalyst particles derived from 0.1 M NH_4VO_3 -H₃PO₄-citric acid solution, and (F) Y_2O_3 -stabilized ZrO_2 discontinuous fiber derived from ZAC-6 wt% PVOH-surfactant solution.

Part 1: Nanoparticle Synthesis – Vapor Phase Synthesis

Spray Pyrolysis: $\text{Ga}(\text{NO}_3)_3$ and GaN

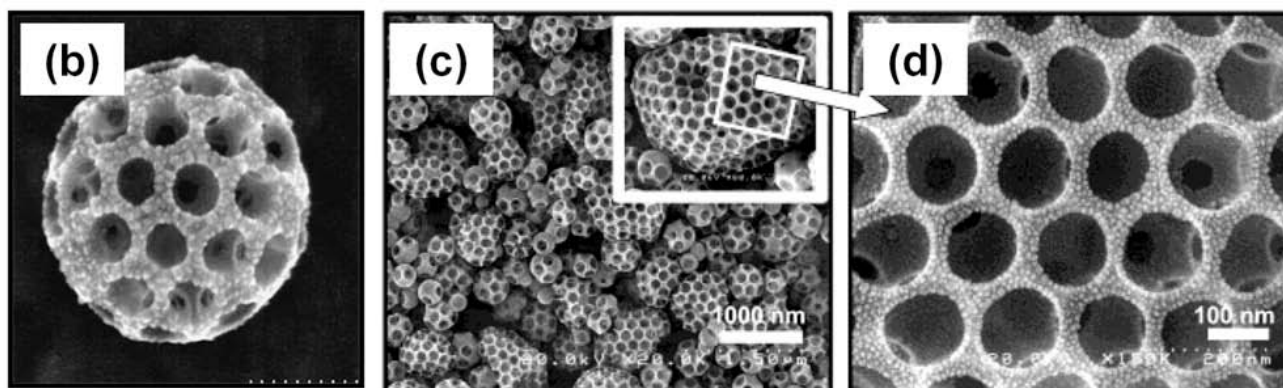
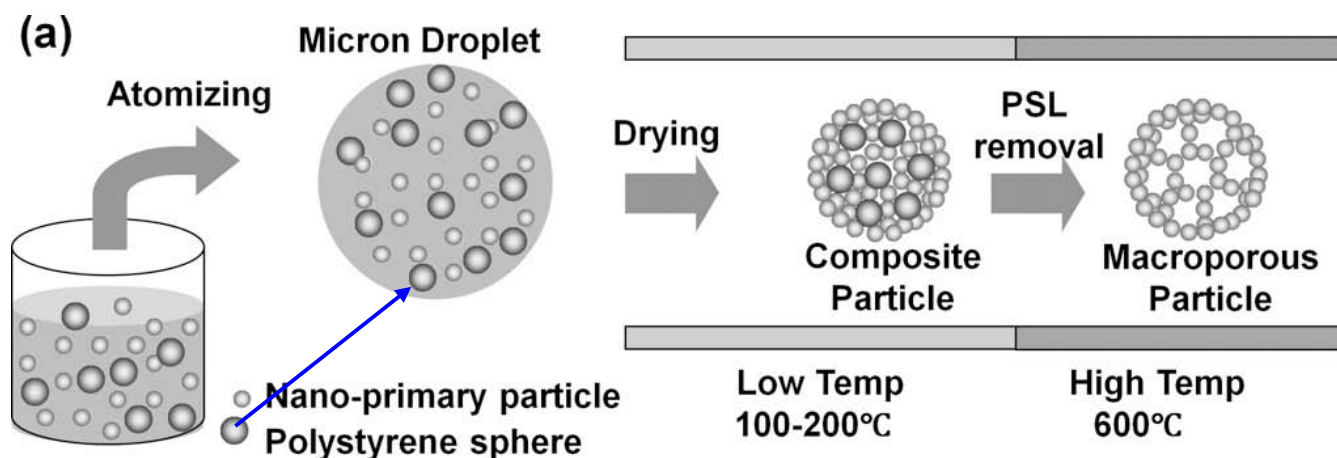


GaN nanoparticles of
 23.4 ± 1.7 nm diameter

T. Ogi et al., Adv. Powder Technology 20 (2009) 29

Spray Pyrolysis: Porous Silica NP

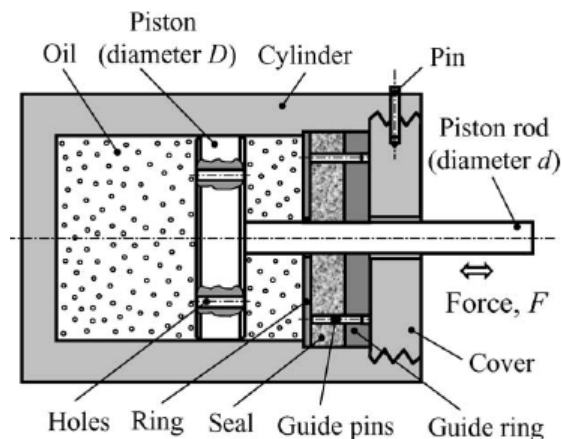
Pyrolysis: Generate droplet mixtures of “Primary Particles” with Polymer Particles



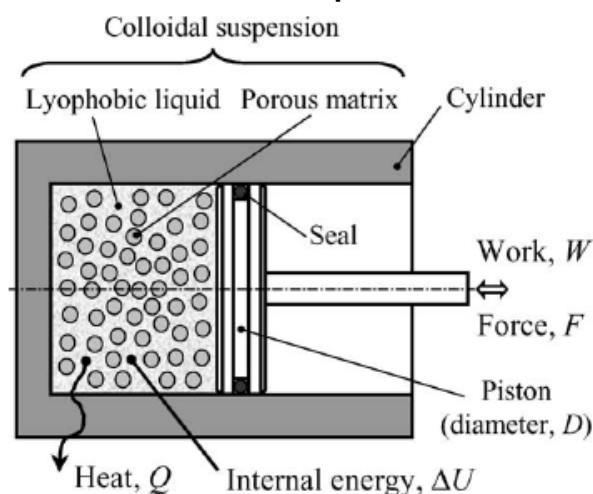
F. Iskandar / Advanced Powder Technology 20 (2009) 283

Porous Silica NP Application: Colloidal Damper

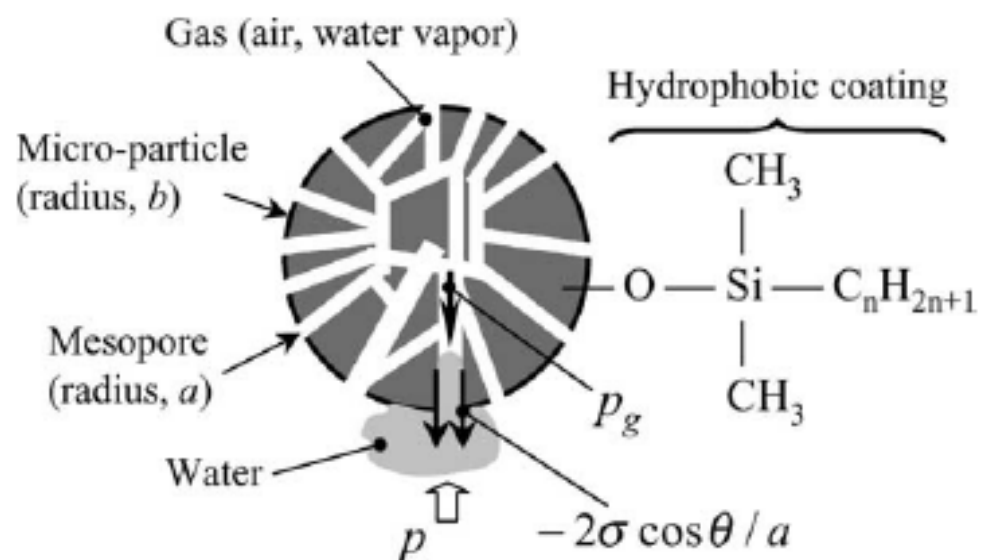
Hydraulic Damper (oil is working fluid, energy is dissipated via orifice flow)



Colloidal Damper



Hydrophobized porous silica particle (outside and inside) suspended in water as the working fluid



Advantage: Little heat generation in colloidal damper.

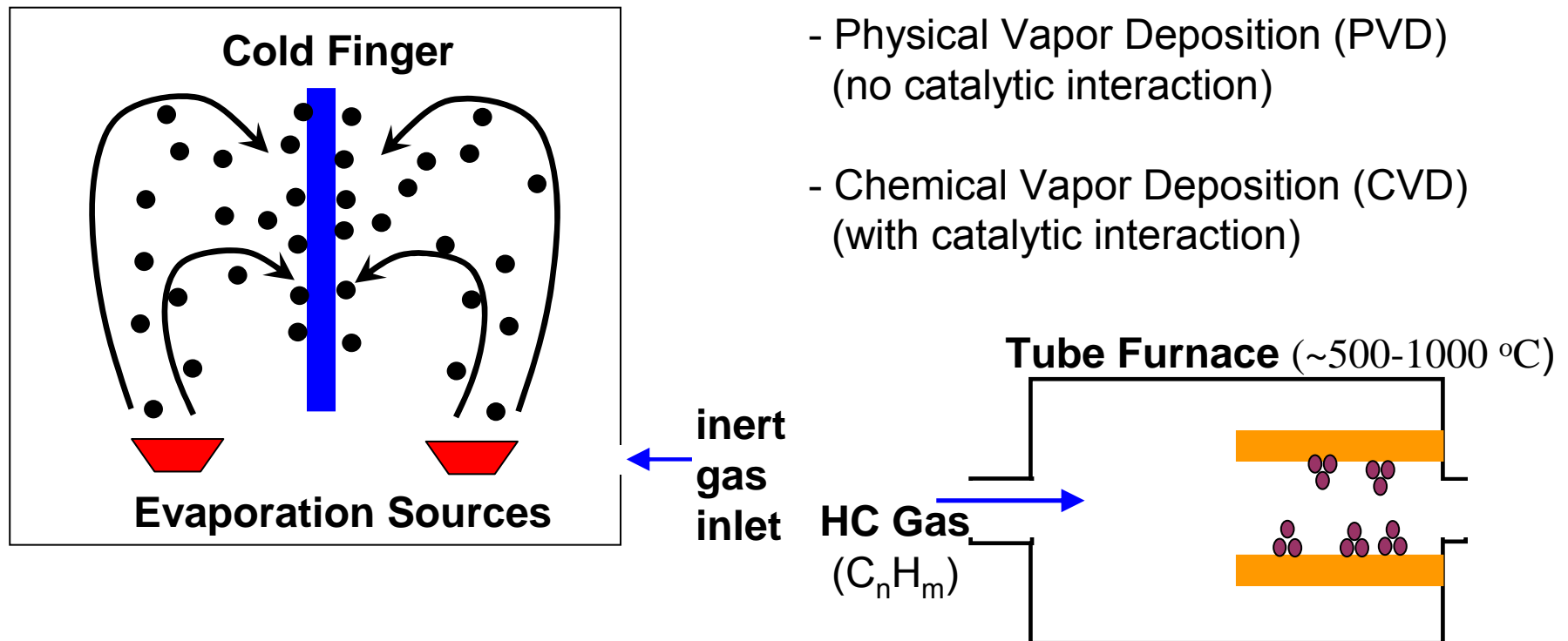
C.V. Suci et al., J. Coll. Interf. Sci., 259 (2003) 62.

Inert Gas Condensation (IGC)

Entails the evaporation of a course substance in an inert gas atmosphere.

Methods:

- Physical Vapor Deposition (PVD)
(no catalytic interaction)
- Chemical Vapor Deposition (CVD)
(with catalytic interaction)



F. Iskandar, Adv. Powder Techn. **20** (2009) 283

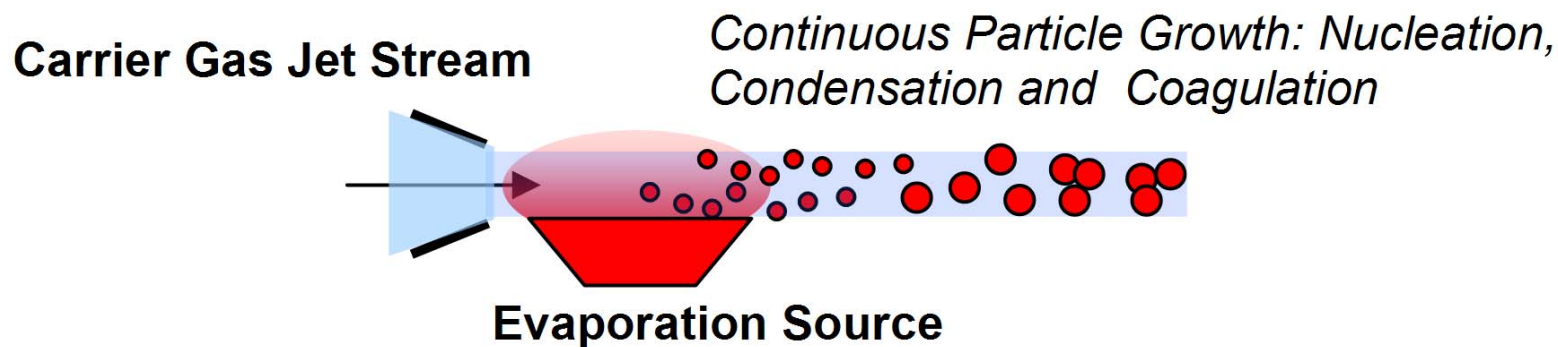
Coalescence and Agglomeration

One of the big challenges in condensation growth is that the particles coalesce and agglomerate.

A solution proposed: **Use of a gas jet stream.** A jet stream of carrier gas positioned above the evaporation sites is used to carry away the metal vapor.

Utilize that carrier gas vapor mixture cools downstream

→ **Continuous Particle growth**
(nucleation, condensation and coagulation)



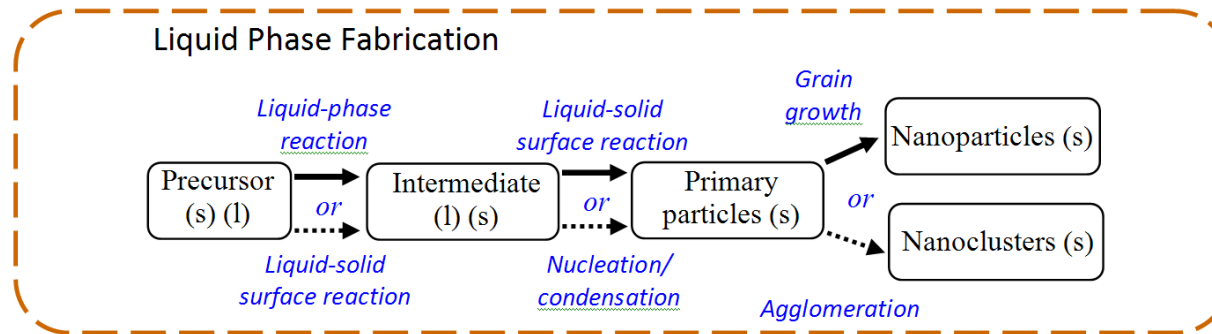
Liquid Phase Synthesis Methods

The liquid phase fabrication entails a wet chemistry route.

Methods:

- Solvothermal Methods
(e.g. hydrothermal)
- Sol-Gel Methods
- Synthesis in Structure Media
(e.g., microemulsion)

Mechanism and Effectiveness



- (i) precursor solution (typically involves a catalyst)
- (ii) nucleation, and
- (iii) growth stage

Effectiveness demands:

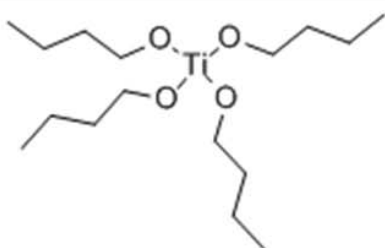
- simple process
- low cost
- continuous operation
- high yield

Sol-Gel and Solvothermal Synthesis

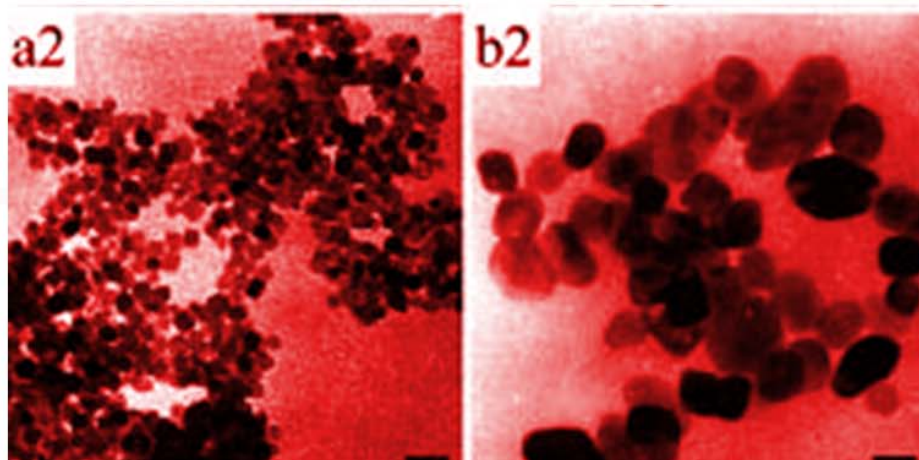
Solvothermal Synthesis

- Precursors are dissolved in hot solvents (e.g., n-butyl alcohol)
 - Solvent other than water can provide milder and friendlier reaction conditions. If the solvent is water then the process is referred to as hydrothermal method.

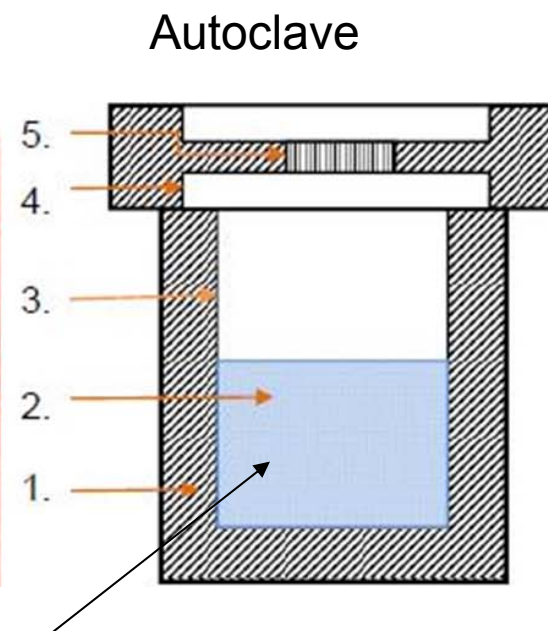
Precursor:
Titanium
n-butoxide



Example: TiO_2 Nanocrystallites



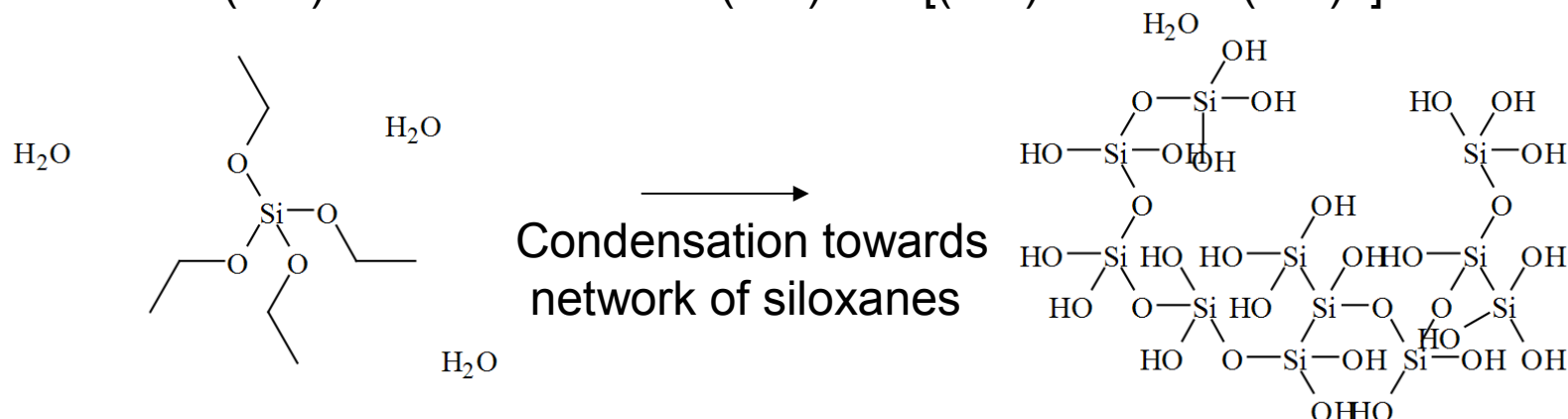
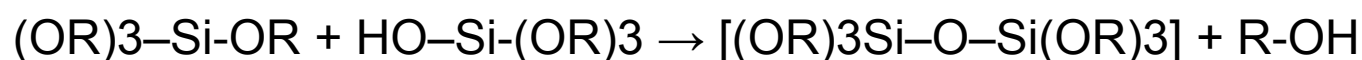
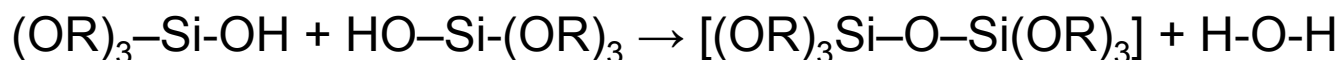
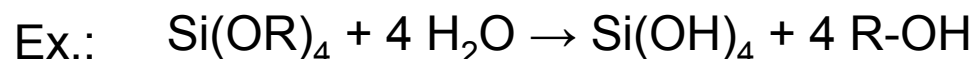
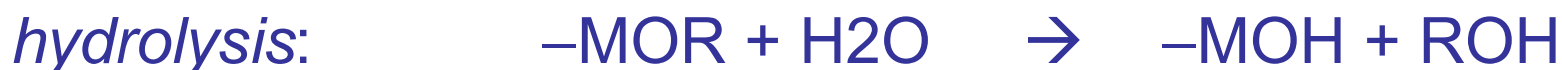
X.F. Yang et al., Euro. J. Inorganic Chem., 2229 (2006).



Precursor solution with butyl alcohol

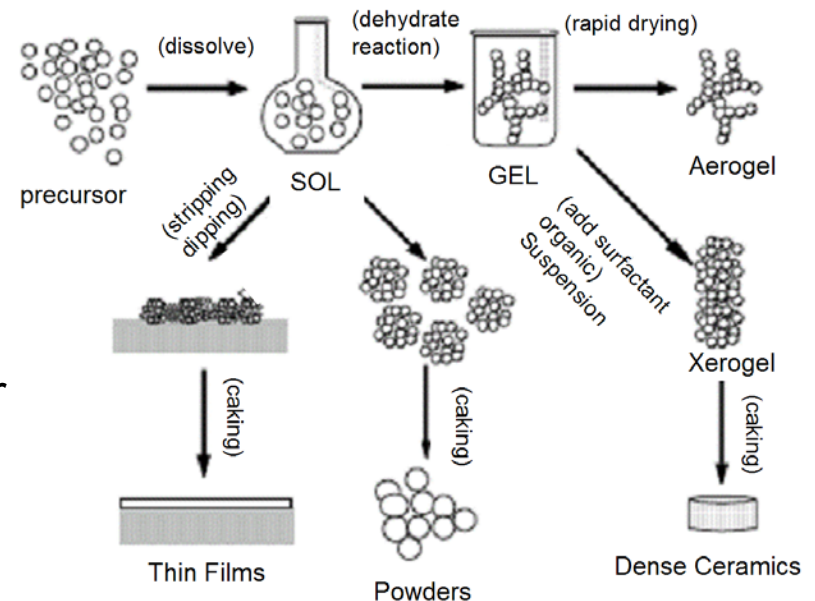
Sol-Gel Processing

- Creation of Sol (solid particles in solution)
- Followed by the following two generic sol-gel processes (assuming as a precursor a metal alkoxide MOR):



Sol-Gel Steps:

- Formation of stable sol solution
- Gelation via a polycondensation or polyesterification reaction
- Gel aging into a solid mass. → causes contraction of the gel network, also
 - (i) phase transformations and
 - (ii) Ostwald ripening.
- Drying of the gel to remove liquid phases. Can lead to fundamental changes in the structure of the gel.
- Dehydration at temperatures as high as 8000 °C, used to remove M-OH groups for stabilizing the gel, i.e., to protect it from rehydration.
- Densification and decomposition of the gels at high temperatures ($T > 8000$ °C), i.e., to collapse the pores in the gel network and to drive out remaining organic contaminants

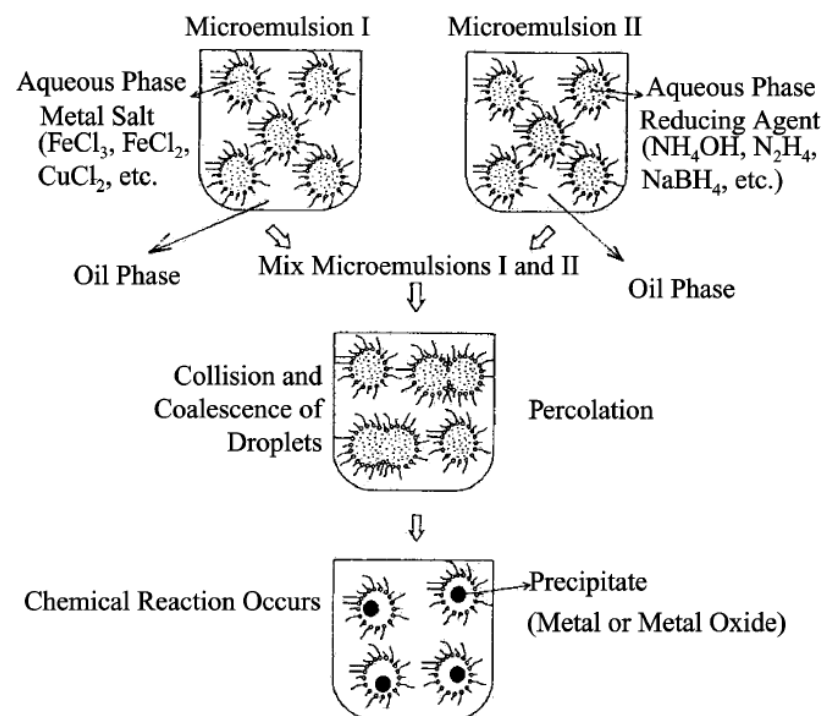


Synthesis in Structured Medium

Influence Growth Kinetics by Imposing Constraints
in Form of Matrices:

- Zeolites
- Layered Solids
- Molecular Sieves
- Micelles/Microemulsions
- Gels
- Polymers
- Glasses

Ex.: Mixing of two Microemulsion
carrying metal salt and reducing agent



I. Capek, Adv. Coll. Interf. Sci. 110 (2004) 49

→ Intermicellar interchange process via coalescence (rate limiting)
(much slower than diffusion: 10 μ s and 1 ms)

NP Systems: Unique Properties

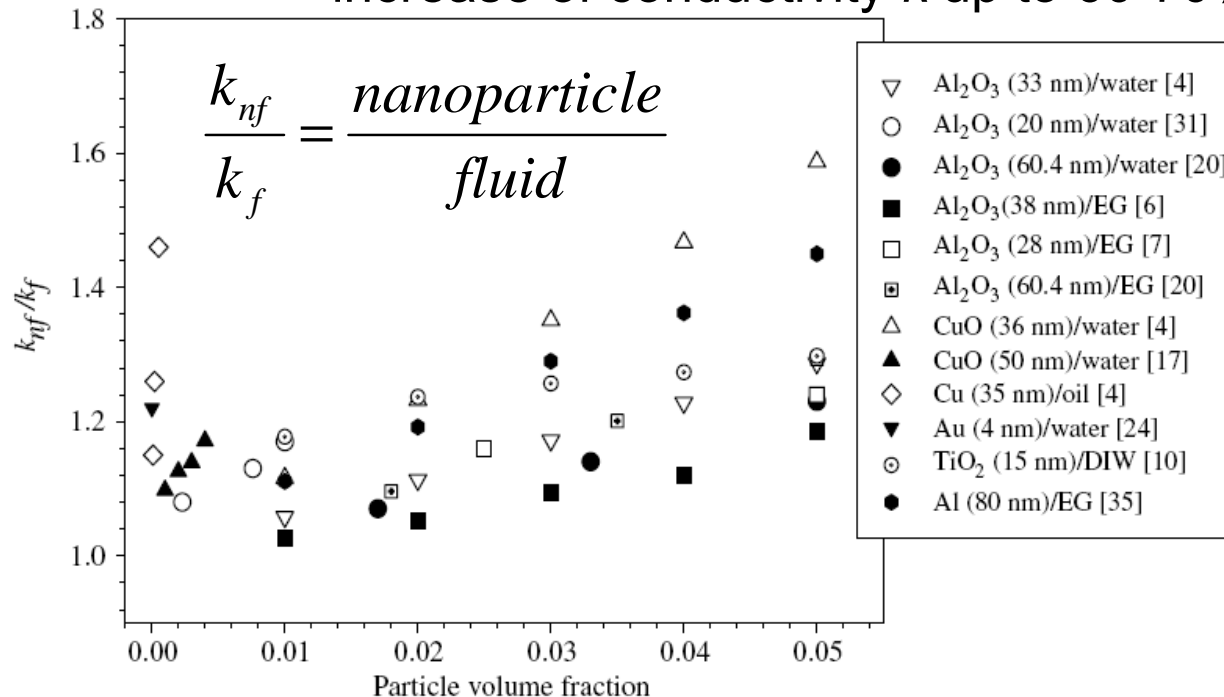
Optics:	High- or low refractive index
Electronics:	Unique density of state
Catalysis:	High reactivity
Drug Delivery:	Controlled delivery
Sensors:	High sensitivity
Coatings:	Increased material strength Ultralow and high adhesion

High impact on composite and fluidic systems.

Nanofluids: High Thermal Conductivity

Nanofluids: Nanoparticle suspension

increase of conductivity k up to 60-70%



Maxwell Model :
$$k_{nf} = k_f \left(\frac{k_p + 2k_f + 2\phi(k_p - k_f)}{k_p + 2k_f - \phi(k_p - k_f)} \right)$$

k_p, k_f particle and fluid thermal conductivity,
 ϕ particle free volume fraction

Such classical models cannot account for increased conductivity in nanofluids.

Nanofluids: High Thermal Conductivity

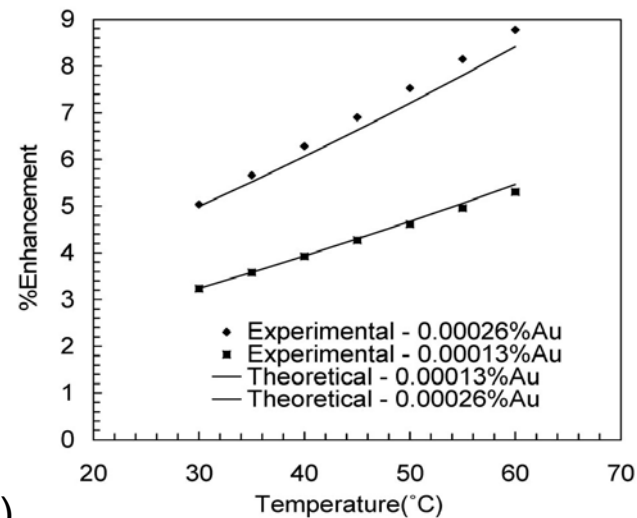
Classical models cannot account for increased conductivity in nanofluids as they lack information about:

- Particle size and surface energy
- Particle dispersion and clustering
- Brownian motion of the particles
- Liquid layering (entropy reduction)
-

Dynamic Model (based on kinetic theory and Fourier's Law) considers Brownian motion and particle size:

$$k_{nf} = k_f \left(1 + c \frac{2k_B T}{\pi \eta d_p^2} \frac{\phi r_f}{(1 - \phi) r_p} \right)$$

D.H. Kumar et al., Phys. Rev. Lett. **93** (2004) 4301)



Nanofluids: Conduction Models

Murshed argues:

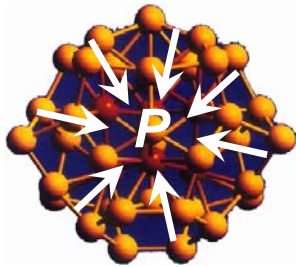
- Most of the recently developed models only include one or two postulated mechanisms of nanofluids heat transfer.
- Moreover, these models were not validated with a wide range of experimental data.
- There is, therefore a need to develop more comprehensive models, which are based on the first principle, and can explicitly explain the enhanced thermal conductivity of nanofluids.
- Particles size, particle dispersions and clustering should be taken into account in the model development for nanofluids.

Researchers	Models/Expressions for nanofluids
Wang et al. [17]	$\frac{k_{eff}}{k_f} = \frac{(1-\phi) + 3\phi \int_0^\infty \frac{k_{sf}(r)n(r)}{k_{sf}(r) + 2k_f} dr}{(1-\phi) + 3\phi \int_0^\infty \frac{k_{sf}(r)}{k_{sf}(r) + 2k_f} dr}$
Xue [60]	$9\left(1 - \frac{v}{\lambda}\right) \frac{k_{eff} - k_f}{2k_{eff} + k_f} + \frac{v}{\lambda} \left[\frac{k_{eff} - k_{c,x}}{k_{eff} + B_{2,x}(k_{c,x} - k_{eff})} + 4 \frac{k_{eff} - k_{c,y}}{2k_{eff} + (1 - B_{2,x})(k_{c,y} - k_{eff})} \right] = 0$
Yu and Choi [38,61]	$(1) \quad k_{eff}/k_f = \frac{k_{pe} + 2k_f + 2\phi(k_{pe} - k_f)(1 + \beta)^3}{k_{pe} + 2k_f - \phi(k_p - k_f)(1 + \beta)^3}$ $(2) \quad k_{eff}/k_f = 1 + \frac{n\phi_{eff}A}{1 - \phi_{eff}A}, \text{ where } A = \frac{1}{3} \sum_{j=a,b,c} \frac{k_{pj} - k_f}{k_{pj} + (n-1)k_f}$
Xuan et al. [62]	$k_{eff}/k_f = \frac{k_p + 2k_f - 2\phi(k_f - k_p)}{k_p + 2k_f + \phi(k_f - k_p)} + \frac{\phi \rho_p c_p}{2k_f} \sqrt{\frac{K_B T}{3\pi v_c \eta}}$
Kumar et al. [24]	$k_{eff}/k_f = 1 + c \frac{2K_B T}{\pi \eta d_p^2} \frac{\phi r_f}{k_f(1 - \phi)r_p}$
Jang and Choi [40]	$k_{eff}/k_f = 1 + c \frac{d_f}{d_p} k_f \phi Re_{dp}^2 Pr$
Prasher et al. [63]	$k_{eff}/k_f = (1 + A \phi Re^m Pr^{0.333})^{\frac{(1+2\alpha) + 2\phi(1-\alpha)}{(1+2\alpha) - \phi(1-\alpha)}} \text{ where } \alpha_f = 2R_p k_{ff}/d_p$
Koo and Kleinstreuer [64]	$k_{eff}/k_f = \frac{k_{MG}}{k_f} + \frac{1}{k_f} 5 \times 10^4 \beta \phi \rho_p c_p \sqrt{\frac{K_B T}{\rho_p D}} f(T, \phi)$
Xie et al. [65]	$k_{eff}/k_f = 1 + 3\Theta \phi + \frac{2\Theta^2 \phi^2}{1 - \Theta \phi}$
Gao and Zhou [66]	$1 - \phi = \left(\frac{k_f}{k_{eff}}\right)^{3A} \left(\frac{k_f + B_1}{k_{eff} + B_1}\right)^{3C_1} \left(\frac{k_f + B_2}{k_{eff} + B_2}\right)^{3C_2}$
Leong et al. [67]	$k_{eff} = \frac{(k_p - k_u)\phi_p k_u [2\gamma_1^2 - \gamma^3 + 1] + (k_p + 2k_u)\gamma_1^3 [\phi_p \gamma^3 (k_{lr} - k_f) + k_f]}{\gamma_1^3 (k_p + 2k_u) - (k_p - k_u)\phi_p [\gamma_1^3 + \gamma^3 - 1]}$
Murshed et al. [29]	$k_{eff} = \frac{k_f \left[1 + 0.27 \phi_p^{4/3} \left(\frac{k_p}{k_f} - 1 \right) \right] \left[1 + \frac{0.52 \phi_p}{1 - \phi_p^{1/3}} \left(\frac{k_p}{k_f} - 1 \right) \right]}{1 + \phi_p^{4/3} \left(\frac{k_p}{k_f} - 1 \right) \left(\frac{0.52}{1 - \phi_p^{1/3}} + 0.27 \phi_p^{1/3} + 0.27 \right)}$
Murshed et al. [35]	$k_{eff} = \frac{(k_p - k_u)\phi_p k_u [\gamma_1^2 - \gamma^2 + 1] + (k_p + k_u)\gamma_1^2 [\phi_p \gamma^2 (k_u - k_f) + k_f]}{\gamma_1^2 (k_p + k_u) - (k_p - k_u)\phi_p [\gamma_1^2 + \gamma^2 - 1]}$

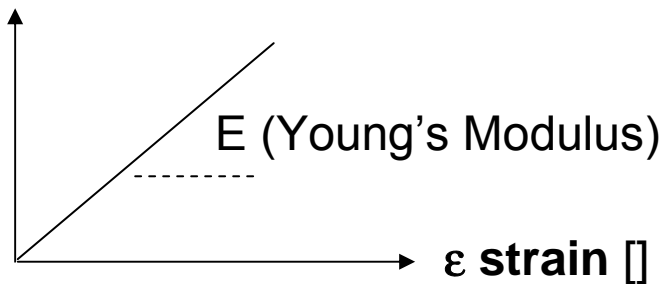
S.M.S. Murshed et al. / Applied Thermal Engineering 28 (2008) 2109–2125

Strain in Nanoparticles

High surface energy (tension) causes strain in the material



σ stress
[GPa]




$$\varepsilon = \frac{\sigma}{E}$$

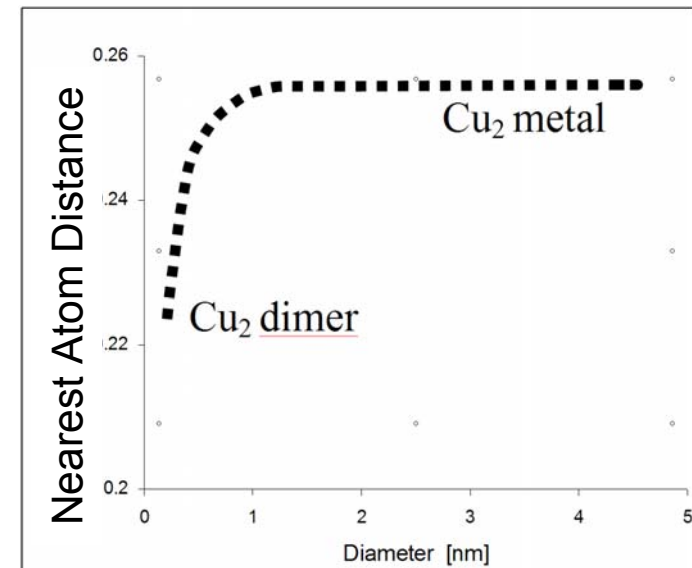
Isotropic stress: $\sigma = 1/3 P$

Pressure caused by interfacial tension:

$$P = 2\gamma/r \quad \dots \text{ Laplace Pressure}$$

γ Surface Tension, r Particle Radius


$$\varepsilon = \frac{1}{3} \frac{P}{E} = \frac{2}{3} \frac{\gamma}{Er} \propto \frac{1}{r}$$



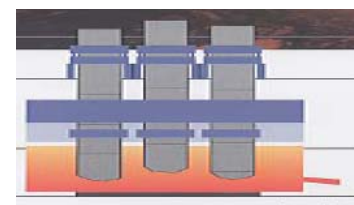
Bulk Crystal and Heterostructure Growth

Nanotechnology needs: Ultrahigh Quality and Purity

E.g., **Crystalline Silicon**: impurity levels < 0.1 ppb (1 in 10¹⁰)

Three Step Process to obtain **Polycrystalline Silicon**:

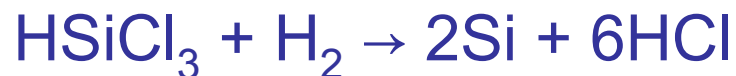
using amorphous carbon electrodes in submerged arc furnace
and carbon in the form of mineral carbon, petroleum coke,
charcoal, wood-chips



additional reduction reactions with dry hydrochloric acid to drive out impurities



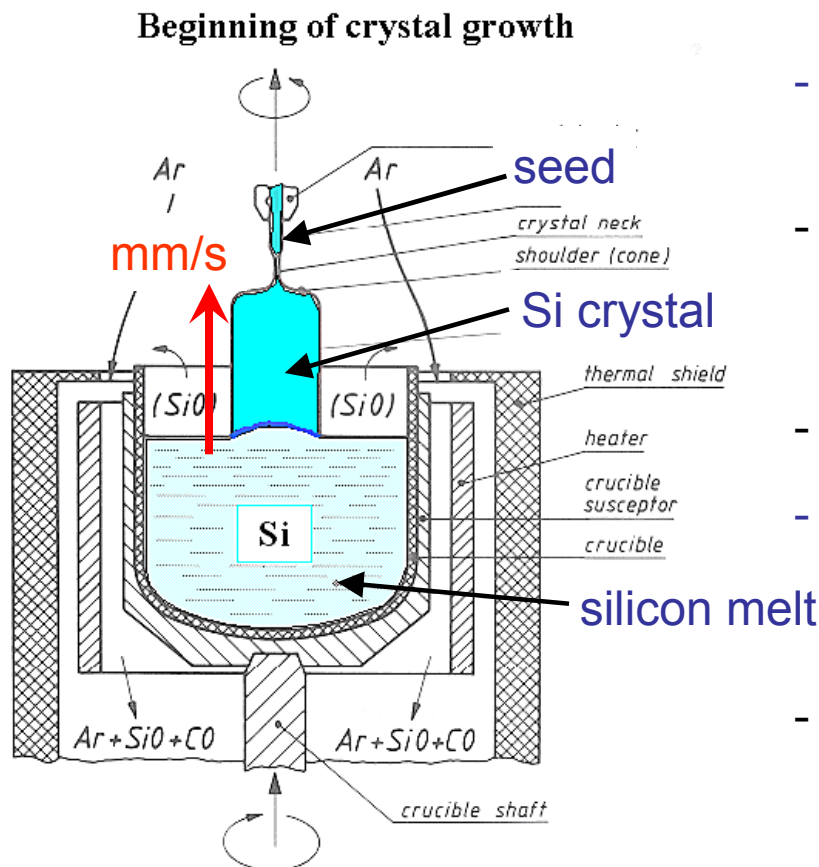
final step: hydrogen conversion reaction of trichlorosilane



Fabrication of Silicon in Nanoelectronics

Polycrystalline silicon conversion into single crystal Si ingots:

Czochralski method: *Yields doped single crystal Si*



- poly-Si crushed in a crucible in clean room and melted
- Convective streams within the melt due to temperature gradients are suppressed by big magnetic fields.
- Dopants added to the melt at this point.
- A seed crystal is inserted and slowly withdrawn (mm/s) under rotational motion to assure homogeneity,
- Via mechanical processes wafers are obtained from the single-crystal ingot.

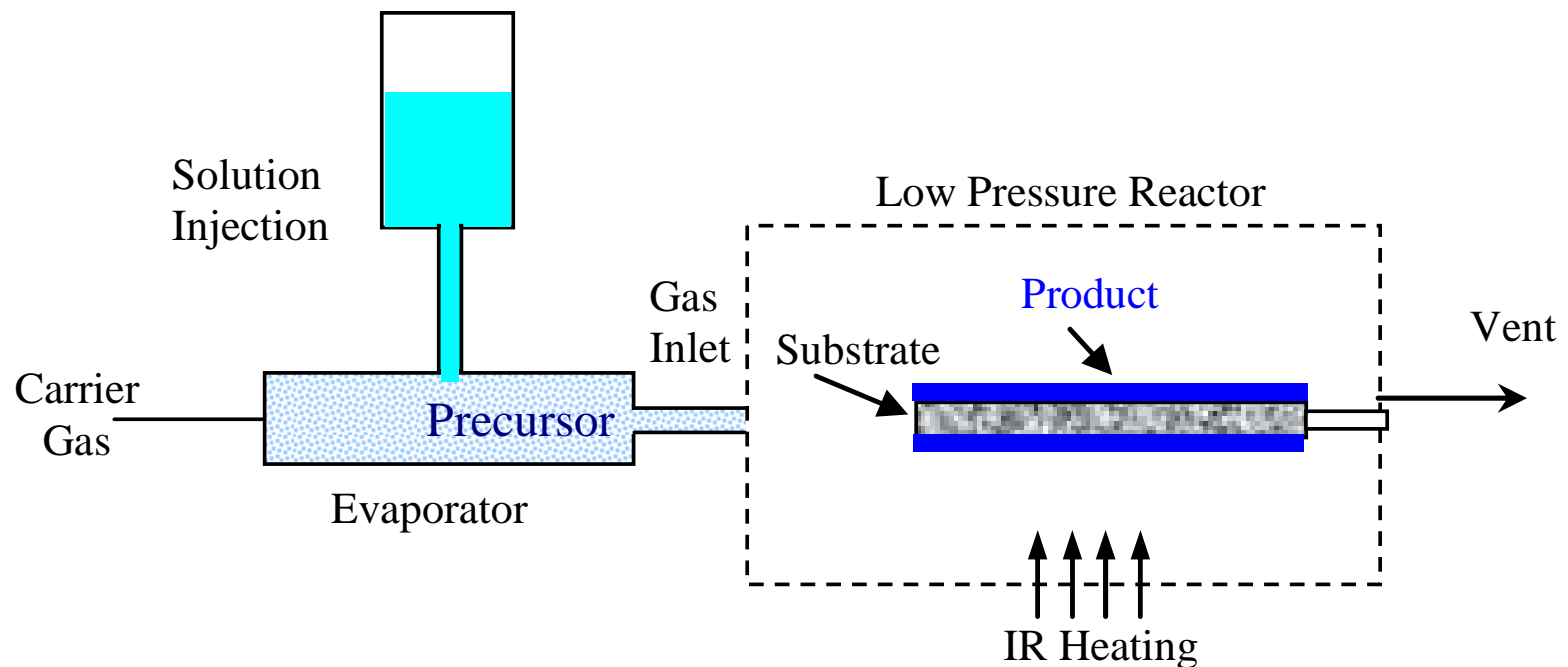
Source: http://www.tf.uni-kiel.de/matwis/amat/elmat_en/kap_6/illustr/i6_1_1.html

Fabrication of Multilayered Crystals

Methods excellently suited for heterostructure growth:

- Chemical Vapor Deposition (CVD)
- Molecular beam epitaxy (MBE)

Schematic of one of many CVD setups



E.g. for silicon layer growth on silicon wafer with dopants: $\text{SiCl}_4 + 2\text{H}_2 \rightarrow \text{Si} + 4\text{HCl}$

Heteroepitaxial Crystal Growth Modes

Three Growth Modes for Heteroepitaxial Growth:

- Frank-van der Merwe (FM) (“layer-by-layer” growth)
- Volmer-Weber (VW) (“island” growth), and
- Stranski-Krastanow (SK) (combined “layer-by-layer and island” growth)

Surface Energies:

γ_1 ... substrate

γ_2 ... epilayer

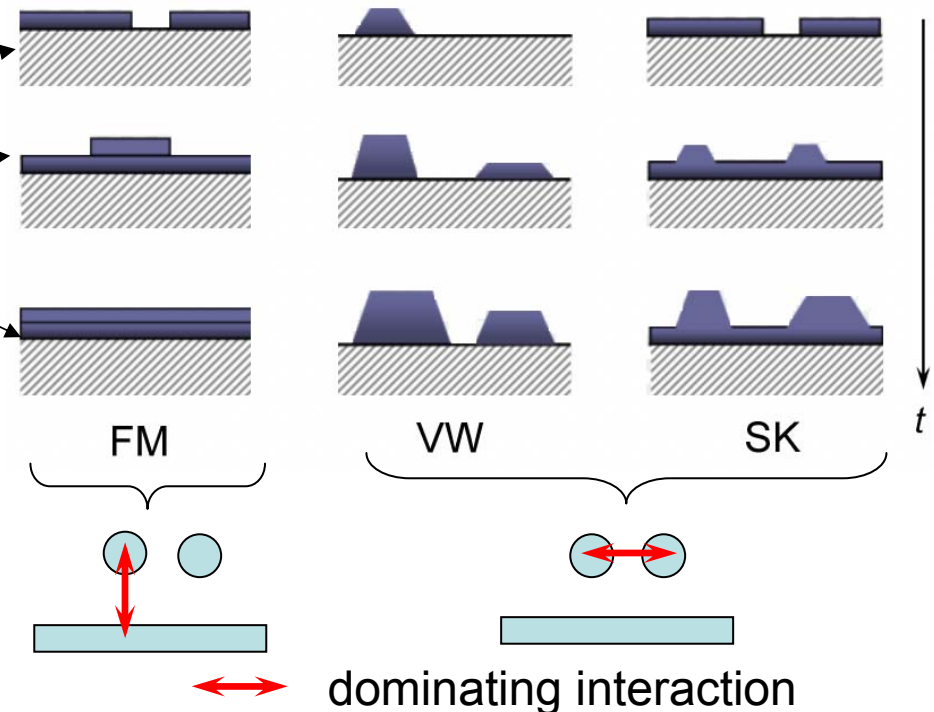
γ_{12} ... interfacial energy

Wetting: $\gamma_1 \geq \gamma_2 + \gamma_{12} \rightarrow \text{FM}$

$$\Delta \gamma \equiv \gamma_2 + \gamma_{12} - \gamma_1 \leq 0$$

“Poor wetting” $\gamma_1 < \gamma_2 + \gamma_{12} \rightarrow \text{VW, SK}$

$$\Delta \gamma \equiv \gamma_2 + \gamma_{12} - \gamma_1 > 0$$



Epilayer (Film) Growth

Chemical Energy of n^{th} monolayer:

$$\mu(n) = \mu_{\infty} + \mu_{\Sigma} = \mu_{\infty} + a^2 [\gamma_2 + \gamma_{12}(n) - \gamma_1] = \mu_{\infty} + a^2 \Delta\gamma$$

μ_{∞} bulk chemical potential of the adsorbate material
 $\mu_{\Sigma} = a^2 \Delta\gamma$ surface chemical potential,

a ... area occupied by an atom

$$\Delta\gamma = \gamma_2 + \gamma_{12}(n) - \gamma_1 \quad \begin{cases} \leq 0; & \text{FM growth} \\ > 0; & \text{VM growth} \end{cases}$$

equivalent to the chemical potential difference of the n^{th} layer and bulk

$$\Delta\mu \equiv a^2 \Delta\gamma = \mu(n) - \mu_{\infty} \quad \begin{cases} \leq 0; & \text{FM growth} \\ > 0; & \text{VM growth} \end{cases}$$

→ Surface energy increases for FM growth (and vice versa)

Epilayer Pseudomorphic Growth

Chemical Energy of n^{th} monolayer with interfacial stress:

$$\mu(n) = \mu_{\infty} + \Delta E^* = \mu_{\infty} + a^2 [\gamma_2 + \gamma_{12}^*(n) - \gamma_1] = \mu_{\infty} + a^2 \Delta \gamma^*$$

$$\gamma_{12}^*(n)$$
$$\Delta \gamma^*$$

thickness dependent interfacial stress or difference

→ ΔE^* , “adhesion energy between misfitting crystals”

$$\Delta E^* = a^2 \Delta \gamma^* = \mu(n) - \mu_{\infty} = [\varphi_{des} - \varphi'_{des}(n) + \varepsilon_d(n) + \varepsilon_e(n)]$$

φ_{des} desorption energy of an adsorbate atom from a wetting layer of the same material

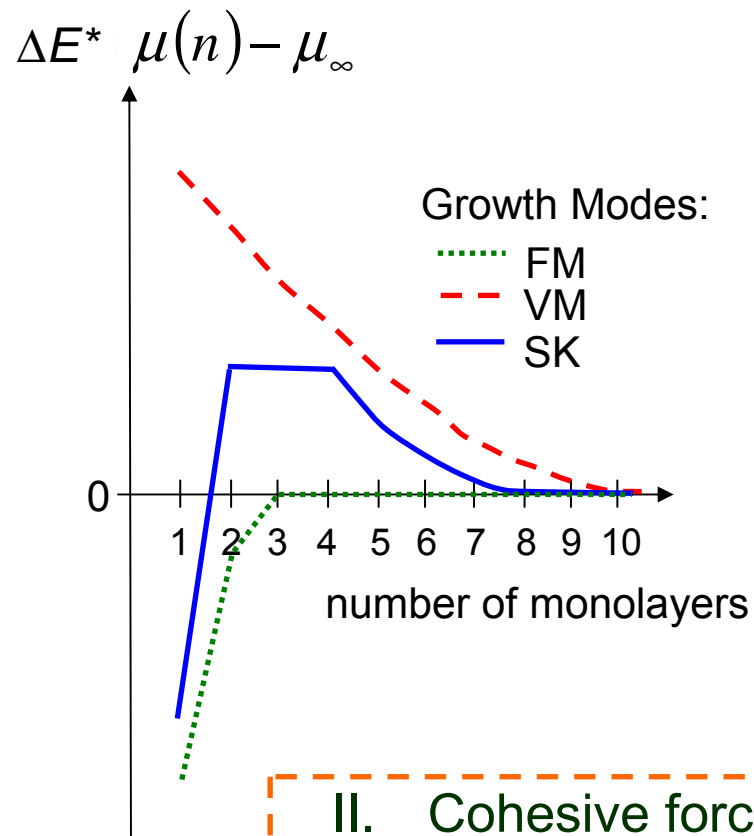
φ'_{des} the desorption energy of an adsorbate atom from the substrate

ε_d the per atom misfit dislocation energy

ε_e the atom homogeneous strain energy, ε_e

$$\Delta E^* = \mu(n) - \mu_{\infty} \approx \begin{cases} \varphi_{des} - \varphi'_{des}(n) & \text{heteroepitaxial} \\ \varepsilon_d(n) + \varepsilon_e(n) & \text{homoepitaxial} \end{cases}$$

Chemical Potential and Growth Modes



I. Adhesive forces exceed cohesive forces

$$\varphi'_{des} > \varphi_{des}$$

and **weak** interfacial mismatch:

→ **Frank-van der Merwe Growth (FM)**

(*Layer-by-layer growth*:

chemical potential increases with increasing layer number)

for **larger** mismatch

→ **Stranski-Krastanov Growth (SK)**

(three growth regimes → *Combined layer-by-layer and island" growth*)

II. Cohesive forces exceed adhesive forces

$$\varphi'_{des} < \varphi_{des}$$

→ **Volmer-Weber Growth (VM)**; i.e., decreasing chemical potential with layer number → *Island growth*